Pergamon

*Journal of Structural Geology*, Vol. 18, No. 4, pp. 451 to 460, 1996

0191-8141/96 $15.00+0.00

0191-8141(95)00097-6

# Experimental and numerical studies of the accommodation of strain incompatibility on the grain scale

Y. ZHANG

CSIRO Exploration and Mining, Private Bag, Wembley, WA 6014, Australia

M. W. JESSELL

Department of Earth Sciences, Monash University, Clayton, Victoria 3168, Australia

and

B. E. HOBBS

CSIRO Exploration and Mining, Private Bag, Wembley, WA 6014, Australia

(*Received* 27 *September* 1994; *accepted in revised form* 31 *July* 1995)

**Abstract**—Strain-incompatibility accommodation mechanisms in polycrystalline deformation have been examined through a comparative study of experimental octachloropropane deformation and correlated numerical modelling. The results show that potential strain incompatibility between neighbouring grains in a deforming polycrystal can be accommodated by diffusive mass transfer, grain boundary migration, intra-grain inhomogeneous deformation and grain boundary sliding. Diffusive mass transfer is capable of relieving space problems in polycrystalline deformation. This process, together with grain boundary migration, prevented the formation of voids and grain overlaps in the deformed octachloropropane polycrystal. Intra-grain and inter-grain inhomogeneous deformations have a different role in maintaining strain compatibility. The former is sufficient in itself to achieve strain compatibility, whereas the latter causes incompatibility problems. Grain boundary sliding is a process capable of effectively accommodating grain interaction. However, this mechanism causes void formation and does not represent a high strain solution by itself.

## INTRODUCTION

It has been widely recognised that large amounts of intragranular plastic deformation can occur in deformed rocks (Turner *et al.* 1954, Schmid *et al.* 1977, Mitra 1978, Mitra & Tullis 1979), metals (Gifkins 1978, Alexander 1985) and laboratory materials (Means 1980, Wilson 1986, Jessell & Lister 1991). When the continuity of a material or the cohesiveness of grain boundaries is maintained after deformation, it is said that the deformation of the material on either side of each boundary is compatible (Means & Jessell 1986). Maintaining this compatibility is believed to be of critical importance to the development of polycrystalline deformation, under conditions where net volume gain is precluded by the confining pressure.

Most geological materials have low crystalline symmetry with anisotropic compliance tensors. In a deforming aggregate with a random distribution of crystallographic orientations, strain incompatibility can arise between neighbouring grains as the strain builds. In order to minimize incompatibility, one or more subsidiary deformation mechanisms must be activated. Understanding these processes will help our understanding of polycrystalline deformation. A number of deformation mechanisms have been recognized from experimentally deformed materials and naturally deformed tectonites, such as intragranular crystalline processes (glide, climb and kinking), diffusive mass transfer, grain boundary sliding and micro-fracturing (Ashby 1970, Ashby & Verrall 1973, Shariat *et al.* 1982, Means & Jessell 1986, Knipe 1989, Lloyd & Knipe 1992). Each of these mechanisms can act as a strain-incompatibility accommodation mechanism, however, any one of these may not be able to accommodate all of the inter-grain strain incompatibility on its own.

In this paper, we aim to examine the accommodation processes of grain-scale strain incompatibility through a comparison between a physical deformation experiment using octachloropropane (OCP) and numerical modelling using a finite difference computer code FLAC (Cundall & Board 1988). The physical experiment was conducted and analysed first. Then the starting geometrical and crystallographic configuration and the deformation boundary conditions, both obtained from the experiment, were used as inputs to the numerical models. Experimental deformation of OCP has been previously investigated by several researchers (Means 1983, Jessell 1986, Means & Ree 1988, Ree 1988, 1990, Jessell & Lister 1991). On the other hand, using FLAC to simulate the deformation of polycrystalline aggregates with one slip system has been attempted by Zhang *et al.* (1993, 1994a,b) and has produced textures similar to those developed in experimentally deformed ice (Wilson & Zhang 1994).

## A DESCRIPTION OF THE TECHNIQUE

### *Analogue experiment*

The specimen of OCP was prepared by mixing a few mg of laboratory grade OCP with a small amount of grinding powder which was used as position markers for tracking deformation development (see Jessell 1986 for a description of the detailed procedure), and is similar to that shown by Jessell & Lister (1991, fig. 2a). Because the main interest of this study is at the grain scale, our observation focused on a small area of the OCP specimen. The enlarged image of the area is illustrated in Fig. 1(a) (outlined by a grid system). This area includes seven grains, labelled as A, B, C, D, E, F and G, which show polygonal grain shapes and smooth grain boundaries and therefore provide an ideal geometry for the later numerical simulation. Using an image analysis method (Bons *et al.* 1993), a grid system was generated for the area, utilizing the marker particles (small black particles in Fig. 1a) introduced in the specimen preparation stage. By observing the change in position of the marker particles before and after deformation, we can measure strain distribution in the deformed OCP specimen.

The experimental deformation of the OCP specimen was carried out at 20°C and at a bulk strain rate of $1.8 \times 10^{-5}\ s^{-1}$ using a torsional deformation rig as described by Jessell & Lister (1991). The microstructure in the deformed sample is shown in Fig. 1(b), the detailed features of which will be discussed later.

### *Numerical experiments*

The next stage of the study was the numerical simulation of the OCP deformation using FLAC. A mesh of $34 \times 34$ elements in size (Fig. 2a) was generated to approximate seven grains in the chosen area of the OCP specimen (Fig. 1a). The slip plane orientations of these grains (Table 1) are derived from the measurements of real OCP lattice orientations, that is basal plane orientations (normal to *c*-axis). As a two-dimensional single slip system model, the trajectories of basal planes on the horizontal plane are considered as the slip directions (Fig. 2b), ignoring *c*-axis plunges out of the plane of the specimen.

Two deformation mechanism scenarios are modelled here. The first is limited to intra-granular slip (dislocation glide) without any grain boundary sliding. Slip on the slip planes is controlled by their critical resolved shear stresses. The second is intra-granular slip plus additional grain boundary sliding (GBS). The theoretical basis for the numerical models has been described in Zhang *et al.* (1993, 1994a,b). The material properties needed to formulate these models (Table 2) were those previously used by Zhang *et al.* (1994a,b).

The boundary conditions used in the model are determined from the starting and final geometries of the chosen area of the OCP specimen area (see Figs. 1a & b). This means that the displacement vectors along the model mesh boundary (Fig. 2c) mimic the changes to the square boundary of the specified area in the OCP specimen. Under this particular boundary condition, the numerical models are constrained to achieve a final boundary geometry identical to that for the OCP experiment.

In the following sections, we will discuss strain-incompatibility accommodation mechanisms by presenting and comparing the experimental and numerical results.

## DIFFUSIVE MASS TRANSFER

As is evident from the final geometry (Fig. 1b), the OCP specimen exhibits micro-structural evidence of deformation. The starting square shape of the area boundary has been deformed into an irregular elongated quadrilateral, and initial polygonal grains with straight grain boundaries have been transformed into elongated grains with irregularly curved boundaries (e.g. grain A, Fig. 1b).

To assess the possibility of involvement of diffusive mass transfer, we have measured local volume variations across different grain boundaries in the chosen area of the deformed OCP specimen. The marker particles contained in OCP crystals are used to define a region across each of the examined grain boundaries (Fig. 3). By calculating the areas of the region before and after deformation, the volume change across each grain boundary can be determined. The measurement revealed that volume changes have occurred at all of the grain boundaries, showing either an increase (volume gain) or a decrease (volume loss). Volume increases are observed for the regions defined across A–C, A–F and A–G boundaries quantified at 5.22, 6.08 and 10.76%, respectively. In contrast, volume decreases are observed for the regions defined across A–B and A–D boundaries: the amounts are −5.53 and −5.68%, respectively. Because a plane strain condition has been maintained throughout the deformation of the OCP specimen, these local volume variations are attributed to the result of diffusive mass transfer operating during the process of deformation. The diffusion leads to migrational flux of the material from a source region to a sink region, therefore resulting in volume losses and gains respectively in these two types of regions.

The current observation of diffusive mass transfer in deforming OCP polycrystals is a support to the report by Ree (1994). Previously, it has been generally assumed that the deformation mechanisms responsible for intra-granular straining of OCP grains are those involving glide systems, including dislocation glide and climb, some kind of combination of glide and climb, kinking

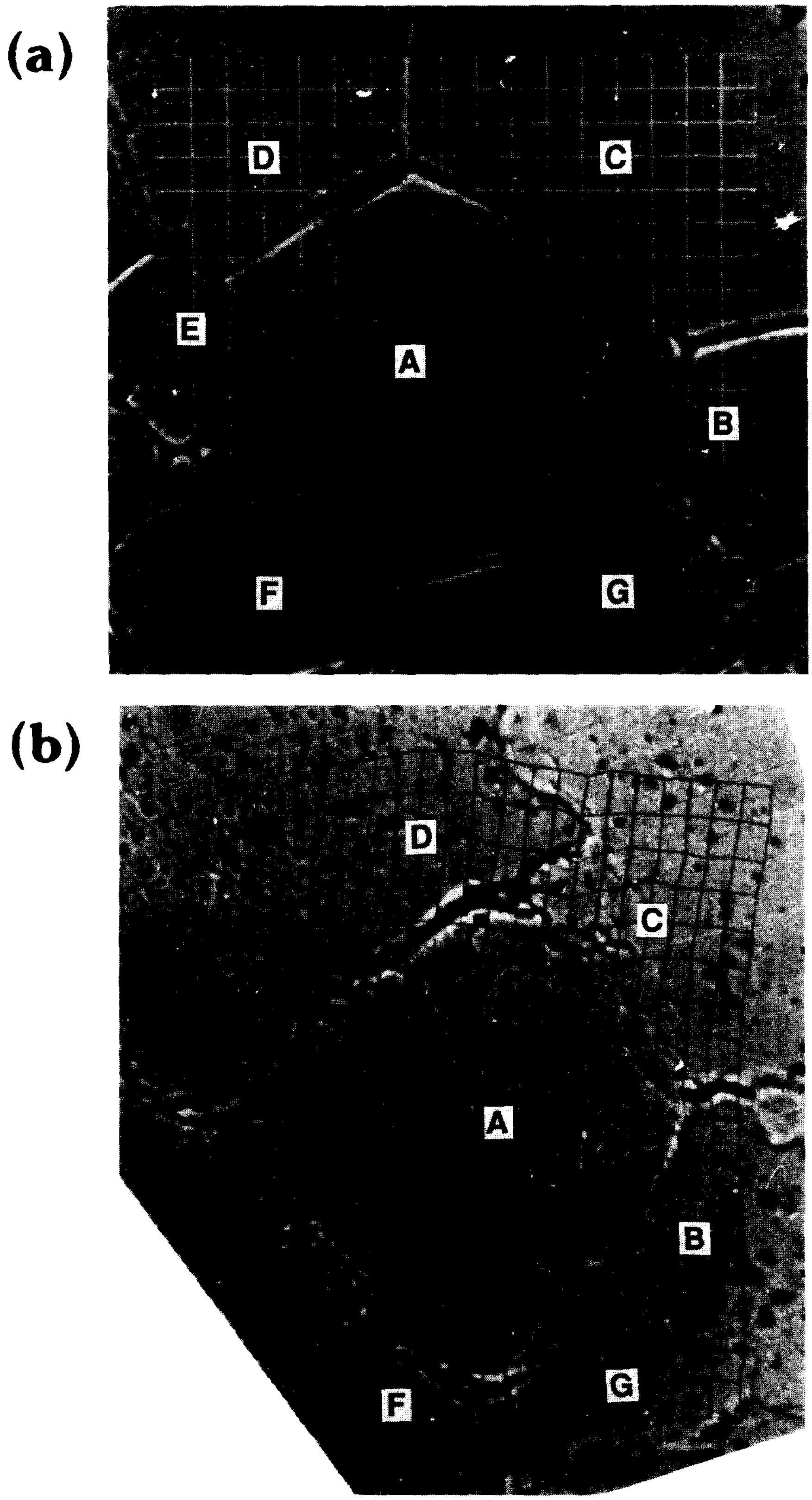


Fig. 1. (a) Plane light photomicrograph of the OCP specimen area chosen for observation and simulations, which is covered by a grid created for later use in strain calculation; the width is about 0.6 mm. (b) Plane light photomicrograph of the initially chosen OCP specimen area after deformation; the distorted grid illustrates real deformation. The grains are labelled by A–G.

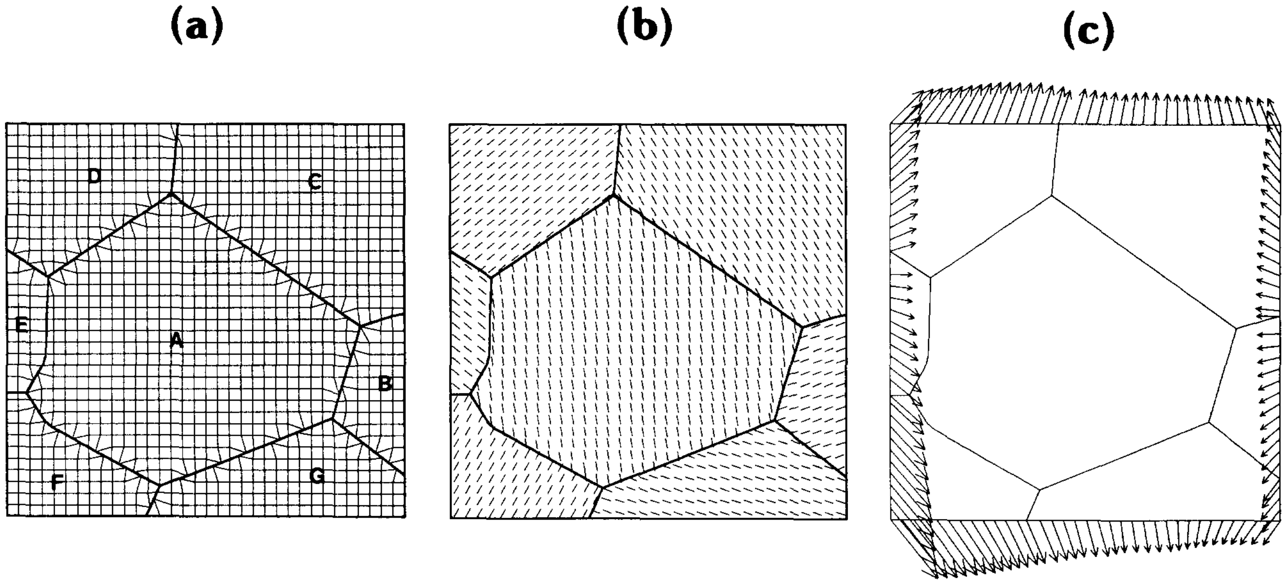


Fig. 2. (a) The starting finite difference mesh for numerical simulations. Marked lines show grain boundaries; note that triangular elements are involved along grain boundaries due to the need to mesh grain boundaries numerically. (b) Initial slip plane traces in the numerical specimen. (c) The displacement rate boundary condition used in numerical simulations. Grain labels (A–G) correspond to those in Fig. 1.

Table 1. Lattice orientations

| Grain | *c*-Axis (measured in OCP sample) | Slip plane (used in FLAC modelling) |
|---|---|---|
| A | 136°*/53°† | 46°‡ |
| B | 106°/59° | 16° |
| C | 96°/43° | 6° |
| D | 46°/49° | 136° |
| E | 2°/51° | 92° |
| F | 128°/10° | 38° |
| G | 1°/53° | 91° |

*Orientation angle of the horizontal projection line of *c*-axis measured anti-clockwise from a reference line which is used as *x*-axis in the FLAC simulation frame (see Zhang *et al.* 1994a).

†*c*-Axis plunge.

‡Orientation angle of trace of the (0001) plane on the plane of the thin section.

Table 2. Material properties

| | | |
|---|---|---|
| Density | 2647 kg $m^{-3}$ | (Clark 1966) |
| Shear modulus | $4.23 \times 10^{10}$ Pa | (Clark 1966) |
| Bulk modulus | $4.64 \times 10^{10}$ Pa | (Clark 1966) |
| Matrix cohesion | $2 \times 10^{10}$ Pa | |
| Slip plane cohesion | $2 \times 10^{5}$ Pa | |
| Matrix and slip plane frictions | 0° | |
| Normal stiffness (Kn) | $1.5 \times 10^{12}$ GPa $m^{-1}$ | |
| Shear stiffness (Ks) | $2.2 \times 10^{6}$ GPa $m^{-1}$ | |
| Grain boundary cohesion | $2 \times 10^{5}$ Pa | |
| Boundary tension strength | $4 \times 10^{5}$ Pa | |
| Grain boundary friction | 0° | |

and twinning (Means 1983, Jessell 1986). In the present situation, the deformed OCP polycrystal probably involves at least one of the above mechanisms—dislocation glide (intra-granular slip), together with the observed diffusive mass transfer. Because of the involvement of diffusive mass transfer, dislocation climb, a deformation mechanism dependent on solid-state diffusion, could also be activated. It is difficult to quantify strain partitioning between diffusive mass transfer and dislocation motions or to identify the dominant mechanism in this particular case. However, we can probably speculate that diffusive mass transfer plays a major role in accommodating inter-grain strain incompatibility which would otherwise lead to lock-up during OCP deformation.

The driving force for diffusive mass transfer has been variously identified as stress and strain energy variations (Means 1983, Bell *et al.* 1986, Wheeler 1987), fluid pressure gradients (Etheridge *et al.* 1984), and thermal energy gradients (Ranalli 1987). In the deformed OCP specimen, the dominant agency causing diffusion is believed to be stress and strain variations in the specimen. Different grains in the OCP aggregate have different lattice orientations and therefore have different strengths. Once the specimen is loaded, each OCP grain will deform according to its own orientation. As grain interactions intensify and stress/strain contrasts between neighbouring grains build up, inter-grain strain incompatibilities will tend to arise. These potential incompatibilities must be accommodated if deformation is to proceed. In our OCP specimen, stress and strain contrasts between different grains at this stage could be large enough to activate diffusive mass transfer, probably along grain boundaries. In summary, the whole process proceeds as follows: bulk deformation gives rise to stress/strain contrast, the contrast activates diffusion, the diffusion accommodates strain incompatibility (also reducing stress/strain contrast) and then the bulk deformation is able to proceed.

Diffusive mass transfer is believed to dominate in regimes where the stress is low enough to prevent intra-grain plastic deformation involving glide systems (Knipe 1989). In a high stress regime, glide system-based deformation mechanisms may be fully able to accommodate major strain (Zaoui 1986). However, local diffusive

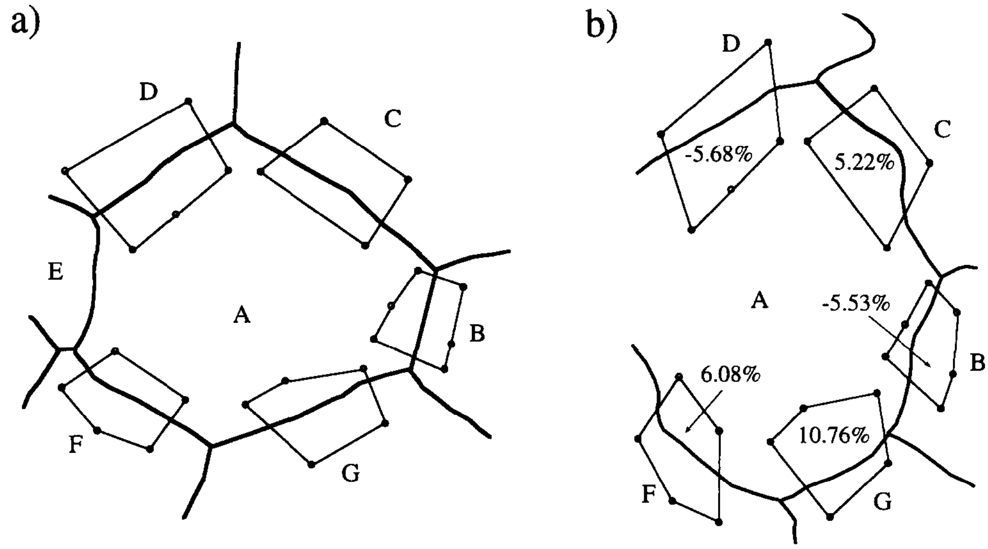


Fig. 3. The geometries of sub-regions defined across grain boundaries before (a) and after (b) deformation, illustrating volume changes (given by percentages). Small circles indicate marker particles and grain labels (A–G) correspond to those in Fig. 1.

mass transfer activated by inter-grain contrast can also operate in this regime. In this case, diffusive mass transfer can be a strain softening mechanism as it facilitates the ability of rock to deform by glide.

## GRAIN BOUNDARY MIGRATION

Grain boundary migration has been observed in the deformed OCP specimen (see Fig. 1b). A common feature is that original straight grain boundaries have all been transformed into highly irregular boundaries. The most significant boundary migration is seen between grains A and E. The migration toward grain E is so large that grain E is totally consumed by grain A. Analyses of the deformed grid (Fig. 4a) and of the positions of marker particles indicate that grain boundary migration is dominated by the change in the positions of grain lattice boundaries rather than of material boundaries, although a certain amount of diffusive mass transfer could also be involved across grain boundaries. This is demonstrated by the fact that grain E disappeared as a lattice independent grain but its material is still there, currently added to grain A.

Grain boundary migration may not be an important strain accommodation mechanism in polycrystalline aggregates since it does not change the relative positions of material points (also see Ree 1990). However, this

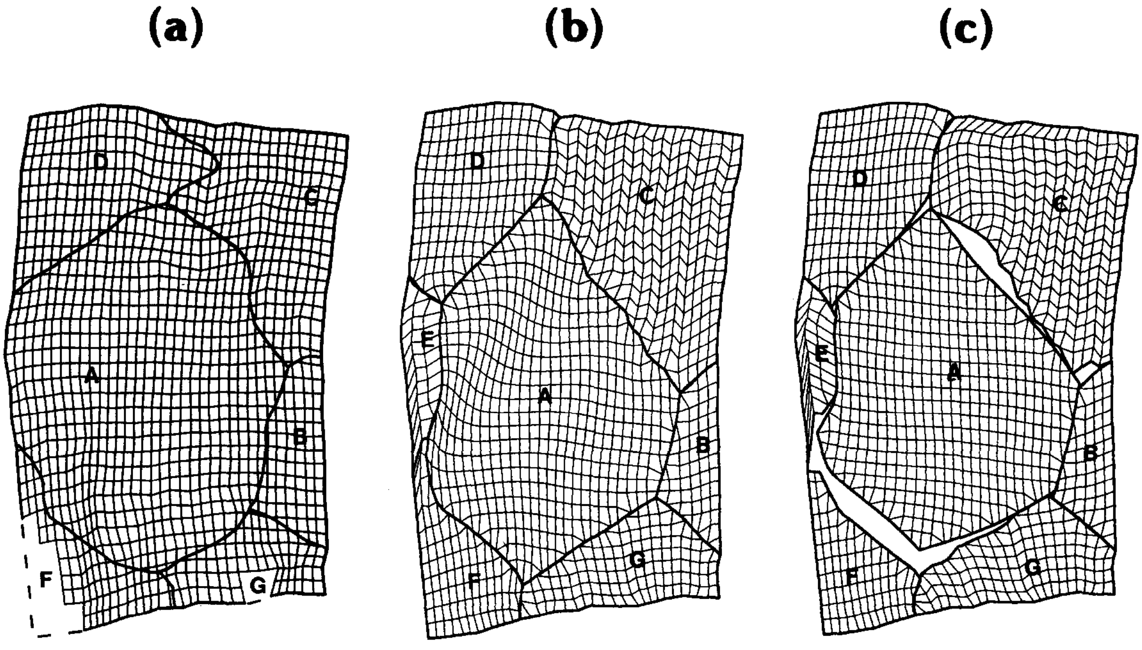


Fig. 4. (a) Deformed grid for the OCP experiment; thick lines mark grain boundaries [grid density is doubled from that shown in Fig. 1(b) through interpolation]. (b) Deformed mesh for the numerical model without grain boundary sliding. (c) Deformed mesh for the numerical model with grain boundary sliding. Grain labels (A–G) correspond to those in Figs. 1 and 2.

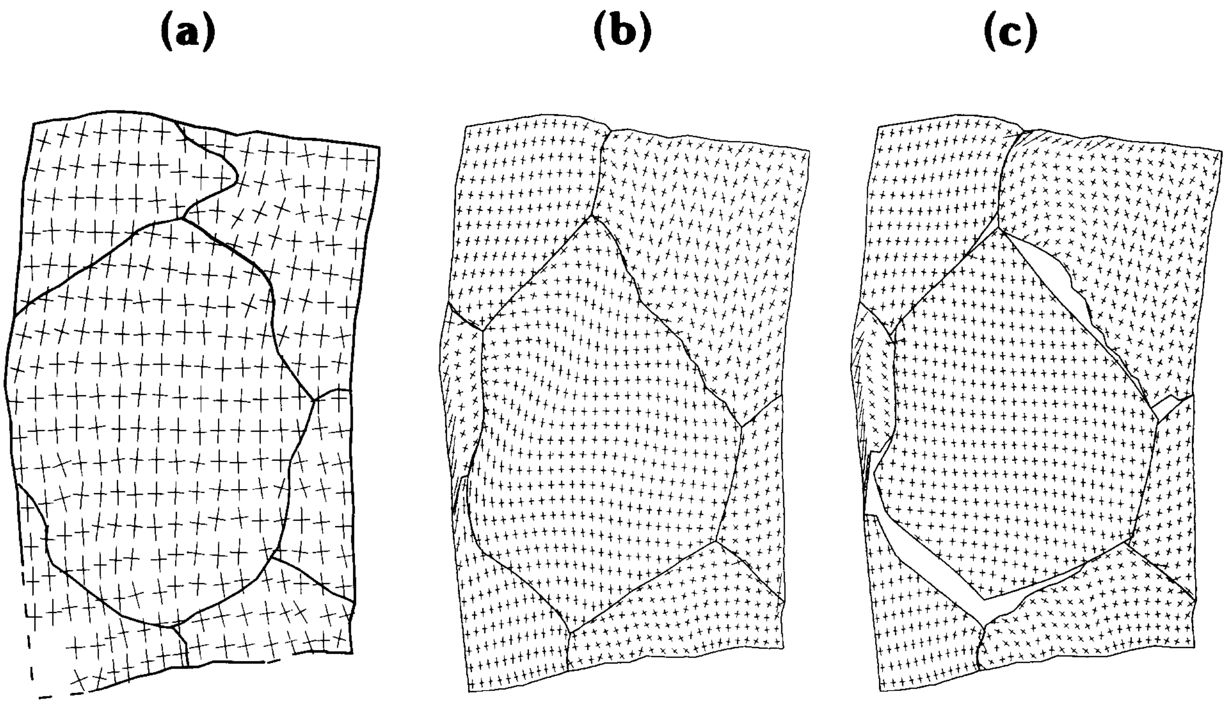


Fig. 5. The distribution of strain ellipse axes for (a) the OCP experiment, (b) the numerical model without grain boundary sliding and (c) the numerical model with grain boundary sliding. See Fig. 3 for grain labels.

process could make some contribution, co-operatively with diffusive mass transfer, to the accommodation of strain incompatibility in the deformed OCP specimen presented here. Because of the contrasting deformation of neighbouring grains and the potential of resulting strain incompatibilities, some grain boundaries may separate areas of different deformation energy on either side and therefore be in an unstable condition. These grain boundaries then need to migrate to relatively stable positions, which gives rise to lattice reorientation across the old grain boundary. This process will help with the accommodation of some strain incompatibility. The dominant driving forces responsible for the migration are probably elastic or plastic strain energy contrast between the grains on either side of the migrated boundary (Jessell 1986, Urai *et al.* 1986).

## INHOMOGENEOUS INTRA-GRAIN DEFORMATION

As pointed out earlier, one of the two numerical models is designed to simulate the operation of intragranular glide on one slip system which follows a critical resolved shear stress criterion (Zhang *et al.* 1993, 1994b). Unlike the experimental approach, this numerical model cannot simulate the diffusive mass transfer and grain boundary migration observed in the deformed OCP specimen, although the starting geometry, lattice orientations and boundary condition in the model are derived from the real experiment. This model reproduces the deformation of the chosen OCP area entirely by glide on one slip system.

Figures 4(b) and 5(b) give the deformed mesh and strain distribution in the deformed numerical specimen. As the initial lattice orientations of the simulated grains are significantly different (Fig. 2b and Table 1) and there is no glide-system-independent deformation mechanism available, the deformation should have been sharply contrasting and strain incompatibility should have arisen between neighbouring grains. However, the results show that strain compatibility is still maintained in the model, as demonstrated by the fact that grain boundaries all remain in contact after deformation. We can see that potential strain incompatibility is accommodated here by intragranular heterogeneous deformation. Through the operation of this mechanism, the interior and the boundary areas of a grain may deform differently. In the interior area, deformation is basically controlled by the lattice orientation of the grain and is relatively independent of its neighbouring grains. In the boundary areas, however, the influence of the surrounding grains become severe. If the deformation at the boundaries was completely controlled by the lattice orientation, strain incompatibility would have arisen and deformation would not have been able to proceed. Therefore, the deformation of the boundary areas of any two neighbouring grains must compromise with each other so that a gradual strain transition is reached toward the boundaries. This feature is particularly clear in the triple junction area between grains A, E and F (Figs. 4b and 5b), where significant heterogeneous strain must take place to accommodate a severe compatibility problem, which was otherwise absorbed by diffusive mass transfer and grain boundary migration in the experimentally deformed OCP polycrystal.

This experiment suggests that inhomogeneous deformation is not always an obstacle to achieving strain compatibility. A clear distinction should be drawn between inter-grain strain inhomogeneity and intra-grain strain inhomogeneity. On the one hand, inter-grain strain inhomogeneity which originates from contrasting deformation of neighbouring grains causes the incompatibility problem, particularly between 'soft' grains and 'hard' grains (Ree 1990, Zhang *et al.* 1994b). On the other hand, intra-grain strain inhomogeneity which emerges as a result of compatibility condition (Zaoui 1986) actually facilitates the maintenance of strain compatibility.

To generate intra-grain strain inhomogeneity as a strain-incompatibility accommodation mechanism in a single slip system model, a number of other glide-plane-based mechanisms must be involved together with gliding. These mechanisms include kinking, lattice bending, twinning, sub-grain formation and climb; of which only the first two mechanisms could occur in this model. Through the operation of all these mechanisms, the direction and amount of gliding can change locally. Furthermore, the possibility of the involvement of intra-grain strain inhomogeneity as an incompatibility accommodation mechanism has a relation to the number of glide systems available in a mineral. If there are five independent slip systems as assumed by some theoretical models (Lister *et al.* 1978), the mutual operation of these systems could be enough to achieve homogeneous deformation. Then there will be no incompatibility problems; this is, of course, unlikely for many real minerals. If glide systems available in a mineral are less than five (perhaps two or three in most situations) (Etchecopar & Vasseur 1987, Harren & Asaro 1989), then intra-grain inhomogeneous deformation becomes a very important mechanism to accommodate strain incompatibility. This is supported by widely observed inter- and intra-grain inhomogeneous strain in deformed rocks (Tullis *et al.* 1973, Mitra & Tullis 1979).

## FRICTIONAL GRAIN BOUNDARY SLIDING

The second numerical model of this study aims to simulate the combination of intragranular glide plus some grain boundary sliding (see Zhang *et al.* 1994a for the model basis). The grain boundary sliding in this study is modelled as mechanical frictional sliding along grain boundaries after grain boundary cohesion is overcome (Knipe 1989, Zhang *et al.* 1994a). This differs from the diffusion-accommodated grain boundary sliding which is generally involved in superplastic flow in metals (Langdon & Vastava 1982, Shariat *et al.* 1982).

Figures 4(c) and 5(c) show the deformed mesh and the strain for the models. Although intra-grain deformation is still significant, grain boundary sliding has been clearly involved in accommodating some bulk deformation. An important distinction from the result of the model without grain boundary sliding (Figs. 4b and 5b) is that deformation within each grain is relatively homogeneous. This is clearly shown, for example, by the much more uniform distortion of grids for grains A and F (Fig. 4c) compared with that for the model without grain boundary sliding (Fig. 4b). A consequence of grain boundary sliding is the formation of inter-grain voids in the specimen after deformation, which is neither observed in the deformed OCP specimen nor allowed in the other numerical model. It is interesting to note that the formation of these voids coincides well with the volume variations observed in the deformed OCP specimen. Grain boundaries A–C, A–F and A–G, where voids are formed, are all boundaries across which volume increase has occurred in the OCP experiment. In contrast, the boundaries of A–B and A–D which do not involve voids formation here all show a volume decrease in the experiment. Volume variations due to diffusive mass transfer (as observed in the physical experiment) could not be modelled, but the boundary condition applied to the numerical model were the same as calculated from the real experiment. Therefore, as grains slide, the boundaries with volume increase in the OCP experiment must show the formation of voids in the model, whereas those with volume decrease in the experiment must be pushed together and remain in contact in the model.

Frictional grain boundary sliding is not sufficient in itself to create large macroscopic deformation (Zhang *et al.* 1994a). This is particularly true for a tightly confined mosaic of hexagonal equi-axed grains without the involvement of mechanisms like diffusion and fracturing (Fig. 6). The simple reason is that there is no space to accommodate the formation of voids, which is a volume-increasing process, and there are no agencies to remove the mutual blocking of neighbouring grains. Intragranular deformation still dominates, producing well-developed lattice preferred orientations (Zhang *et al.* 1994a), and the major role of grain boundary sliding is to accommodate emerging strain incompatibility. In this case, inhomogeneous deformation could also be incorporated to help to accommodate some incompatibility which cannot be taken up by grain boundary sliding (Fig. 6). In natural deformation environments, grain boundary sliding could become the dominant deformation mechanism if extra processes are involved such as diffusion (Gifkins 1976) and fluid flow (Owen 1987). These processes can effectively solve the volume problem and remove the mutual blocking of grains and, therefore, significantly facilitate grain boundary sliding.

## DISCUSSION

It is noted that there is a general coincidence between the deformation results produced by the experimental and numerical approaches. This is demonstrated by comparable strain values (Fig. 5) and roughly similar geometrical features of deformed grids (Fig. 4). For example, the values of grain-average strain for the OCP experiment and the two numerical models are quite close. Grain F consistently shows the highest average strains, with the values of strain ellipticity of 2.04, 2.55 and 2.08 respectively. The other grains all have strain

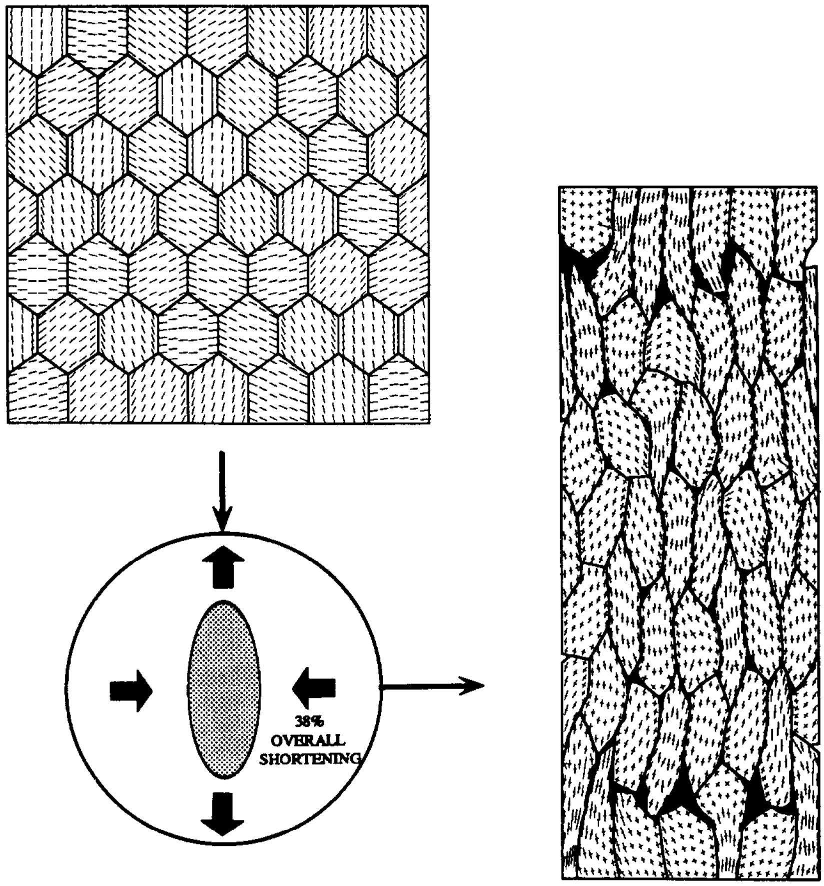


Fig. 6. A numerical model involving grain boundary sliding (see Zhang *et al.* 1994b): initial geometry and lattice orientation (top left), imposed bulk deformation (38% overall shortening) (bottom left) and strain ellipse axis distribution in the deformed specimens (right).

values in the range 1.4–2.0. This consistency suggests that the present numerical approximation, using a polycrystalline aggregate with a single slip system to model OCP, can account for at least an important part of the deformation in real OCP grains.

Despite the similarities mentioned above, differences between the results of the two approaches also exist, dominantly exhibited by grain boundary geometries and the evolution of grain E. Grain boundary migration and diffusive mass transfer in the deformed OCP polycrystal significantly modified grain geometry while accommodating inter-grain strain incompatibility. As a result, original straight boundaries became highly curved, grain E disappeared and grain A grew into a bigger grain. In contrast, these mechanisms are not allowed in the numerical models. Inhomogeneous strain and grain boundary sliding instead acted as incompatibility accommodation mechanisms. Therefore, grain interaction is much stronger than in the situation of OCP deformation, particularly between E and A, where the two grains coexisted and interacted throughout deformation. The other reason possibly responsible for the difference observed here is that OCP grains possess more than one slip system.

It needs to be mentioned that though microfracturing has not been experimentally observed or numerically modelled here, it is an important deformation mechanism at high crustal levels (Sibson 1986, Knipe 1989, Lloyd & Knipe 1992). On a grain scale, microfracturing could be a way to accommodate strain incompatibility. In deforming polycrystals, highest loading or stress most likely occurs along grain boundaries where grains interact and strain incompatibility tends to arise. These locations will first show yield or microfracturing once a breaking point is achieved, thus relieving stress localization and eliminating potential incompatibility. This is probably why inter-grain microfractures usually form at grain contacts, as observed in natural tectonites (Lloyd & Knipe 1992).

## CONCLUSIONS

(1) Strain compatibility is a natural phenomenon of polycrystalline deformation, while incompatibility always tends to arise between neighbouring grains owing to contrasting strengths of grains. This incompatibility can be accommodated by diffusive mass transfer, grain boundary migration, inhomogeneous intra-grain deformation and grain boundary sliding. These processes may not be in themselves the mechanism responsible for the accommodation of major bulk strain.

(2) Diffusive mass transfer, observed along grain boundaries in the deformed octachloropropane specimen, is an important mechanism in relieving space problems while it accommodates inter-grain strain incompatibility. The operation of this mechanism,

together with grain boundary migration, can prevent the formation of overlaps and voids.

(3) Strain inhomogeneity associated with polycrystalline deformation plays a two-fold role in maintaining strain compatibility. While inter-grain strain inhomogeneity causes incompatibility problems, intra-grain inhomogeneity generally accommodates strain incompatibility and facilitates the maintenance of a strain continuum.

(4) Grain boundary sliding is a mechanism capable of accommodating inter-grain incompatibility and achieving geologically 'compatible' deformation. This mechanism, however, causes void formation and does not represent a high strain solution. Its significant involvement needs the help of other processes like diffusive mass transfer.

(5) Further comparison of experimentally observed polycrystalline deformation with numerical simulations is highly desirable. We now have techniques for both and the results will certainly illuminate deformation processes in polycrystals.

*Acknowledgements*—We would like to thank R. J. Norris, W. D. Means, J.-H. Ree and an anonymous referee for their review and critical comments which greatly helped to improve this paper.

## REFERENCES


Alexander, J. M. 1985. On problems of plastic flow of metals. In: *Plasticity Today: Modelling Methods and Application* (edited by Sawczuk, A. & Bianchi, G.). Elsevier, London.

Ashby, M. F. 1970. The deformation of plastically non-homogeneous materials. *Phil. Mag.* **21**, 399–424.

Ashby, M. F. & Verrall, R. A. 1973. Diffusion accommodated flow and superplasticity. *Acta metall.* **21**, 149–163.

Bell, T. H., Rubenach, M. J. & Fleming, P. D. 1986. Porphyroblast nucleation, growth and dislocation in regional metamorphic rocks as a function of deformation partitioning during foliation development. *J. metamorph. Geol.* **4**, 37–67.

Bons, P. D., Jessell, M. W. & Passchier, C. W. 1993. The analysis of progressive deformation of rock analogues. *J. Struct. Geol.* **15**, 403–411.

Clark, S. P. Jr (ed.) 1966. *Handbook of Physical Constants. Geol. Soc. Am. Mem.* **97**.

Cundall, P. A. & Board, M. 1988. A microcomputer program for modelling large-strain plasticity problem. In: *Numerical Methods in Geomechanics* (edited by Swobada, C.). *Proc. 6th Int. Conf. Num. Meth. Geomech.* Balkema, Rotterdam, 2101–2108.

Etchecopar, A. & Vasseur, G. 1987. A 3-D kinematic model of fabric development in polycrystalline aggregates: comparisons with experimental and natural examples. *J. Struct. Geol.* **9**, 705–717.

Etheridge, M. A., Wall, V. J., Cox, S. F. & Vernon, R. H. 1984. High fluid pressures during regional metamorphism and deformation: implications for mass transport and deformation mechanisms. *J. geophys. Res.* **89**, 4344–4358.

Gifkins, R. C. 1976. Grain-boundary sliding and its accommodation during creep and superplasticity. *Met. Trans. A* **7A**, 1225–1232.

Gifkins, R. C. 1978. Grain rearrangements during superplastic deformation. *J. Mater. Sci.* **13** 1926–1936.

Harren, S. V. & Asaro, R. J. 1989. Nonuniform deformation in polycrystals and aspects of the validity of the Taylor model. *J. Mech. Phys. Solids* **37**, 191–233.

Jessell, M. W. 1986. Grain boundary migration and fabric development in experimentally deformed octachloropropane. *J. Struct. Geol.* **8**, 527–542.

Jessell, M. W. & Lister, G. S. 1991. Strain localisation in experimental shear zones. *Pageoph.* **137**, 411–438.

Knipe, R. J. 1989. Deformation mechanisms—recognition from natural tectonites. *J. Struct. Geol.* **11**, 127–146.

Langdon, T. G. & Vastava, R. B. 1982. An evaluation of deformation models for grain boundary sliding. In: *Mechanical Testing for Deformation Model Development* (edited by Rohde, R. W. & Swearengen, J. C.). American Society for the Testing of Materials, Philadelphia.

Lister, G. S., Paterson, M. S. & Hobbs, B. E. 1978. The simulation of fabric development during plastic deformation and its application to quartzite: the model. *Tectonophysics* **45**, 107–158.

Lloyd, G. E. & Knipe, R. J. 1992. Deformation mechanisms accommodating faulting of quartzites under upper crustal conditions. *J. Struct. Geol.* **14**, 127–143.

Means, W. D. 1980. High temperature simple shearing fabrics: a new experimental approach. *J. Struct. Geol.* **2**, 197–202.

Means, W. D. 1983. Microstructure and micromotion in recrystallization flow of Octachloropropane: a first look. *Geol. Rdsch.* **72**, 511–528.

Means, W. D. & Jessell, M. W. 1986. Accommodation migration of grain boundaries. *Tectonophysics* **127**, 67–86.

Means, W. D. & Ree, J.-H. 1988. Seven types of subgrain boundaries in Octachloropropane. *J. Struct. Geol.* **10**, 765–770.

Mitra, S. 1978. Microscopic deformation mechanisms and flow laws in quartzites within the South Mountain anticline. *Tectonophysics* **45**, 129–152.

Mitra, S. & Tullis, J. 1979. A comparison of intracrystalline deformation in naturally and experimentally deformed quartzites. *Tectonophysics* **53**, T21–T27.

Owen, G. 1987. Deformation processes in unconsolidated sands. In: *Deformation of Sediments and Sedimentary Rocks* (edited by Jones, M. E. & Preston, R.). *Spec. Publ. geol. Soc. Lond.* **29**, 11–24.

Ranalli, G. 1987. *Rheology of the Earth: Deformation and Flow Processes in Geophysics and Geodynamics*. Allen & Unwin, Boston.

Ree, J.-H. 1988. Evolution of deformation-induced grain boundary voids in Octachloropropane. *Geol. Soc. Am. Abstr. Progr.* **20**, A213.

Ree, J.-H. 1990. High temperature deformation of octachloropropane: dynamic grain growth and lattice reorientation. In: *Deformation Mechanisms, Rheology and Tectonics* (edited by Knipe, R. J. & Rutter, E. H.). *Spec. Publ. geol. Soc. Lond.* **54**, 363–368.

Ree, J.-H. 1994. Grain boundary deformation and development of grain boundary openings in experimentally deformed octachloropropane. *J. Struct. Geol.* **16**, 403–418.

Schmid, S. M., Boland, J. N. & Paterson, M. S. 1977. Superplastic flow in fine grained limestone. *Tectonophysics* **43**, 257–291.

Shariat, P., Vastava, R. B. & Langdon, T. G. 1982. An evaluation of the roles of intercrystalline and interphase boundary sliding in two-phase superplastic alloys. *Acta metall.* **30**, 285–296.

Sibson, R. H. 1986. Brecciation processes in fault zones—inferences from earthquake rupturing. *Pageoph.* **124**, 159–175.

Turner, F. J., Griggs, D. T. & Heard, H. C. 1954. Experimental deformation of calcite crystals. *Bull. geol. Soc. Am.* **65**, 883–934.

Tullis, J. A., Christie, J. M. & Griggs, D. T. 1973. Microstructures and preferred orientations of experimentally deformed quartzites. *Bull. geol. Soc. Am.* **84**, 294–314.

Urai, J. L., Means, W. D. & Lister, G. S. 1986. Dynamic recrystallization of minerals. In: *Mineral and Rock Deformation: Laboratory Studies* (edited by Hobbs, B. E. & Heard, H. C.). *Am. Geophys. Un. Geophys. Monogr.* **36**, 161–199.

Wheeler, J. 1987. The significance of grain-scale stresses in the kinetics of metamorphism. *Contr. Miner. Petrol.* **17**, 397–404.

Wilson, C. J. L. 1986. Deformation induced recrystallization of ice: the application of in situ experiments. In: *Mineral and Rock Deformation: Laboratory Studies* (edited by Hobbs, B. E. & Heard, H. C.). *Am. Geophys. Un. Geophys. Monogr.* **36**, 213–232.

Wilson, C. J. L. & Zhang, Y. 1994. Comparison between experiment and computer modelling of plane strain simple shear ice deformation. *Glaciology*, **40**, 46–55.

Zaoui, A. 1986. Quasi-physical modelling of the plastic behaviour of polycrystals. In: *Modelling Small Deformations of Polycrystals* (edited by Gittus, J. & Zarka, J.). Elsevier, London, 187–225.

Zhang, Y., Hobbs, B. E. & Jessell, M. W. 1993. Crystallographic preferred orientation development in a buckled single layer: a computer simulation. *J. Struct. Geol.* **15**, 265–276.

Zhang, Y., Hobbs, B. E. & Jessell, M. W. 1994a. The effect of grain boundary sliding on fabric development in polycrystalline aggregates. *J. Struct. Geol.* **16**, 1315–1325.

Zhang, Y., Hobbs, B. E. & Ord, A. 1994b. A numerical simulation of fabric development in polycrystalline aggregates with one slip system. *J. Struct. Geol.* **16**, 1297–1313.